Video Article

Imaging Glioma Initiation *In Vivo* Through a Polished and Reinforced Thin-skull Cranial Window

Lifeng Zhang*, Andree Lapierre*, Brittany Roy, Maili Lim, Jennifer Zhu, Wei Wang, Stephen B. Sampson, Kyuson Yun, Bonnie Lyons, Yun Li, Da-Ting Lin

The Jackson Laboratory

*These authors contributed equally

Correspondence to: Bonnie Lyons at bonnie.lyons@jax.org, Da-Ting Lin at dlin@jax.org

URL: http://www.jove.com/video/4201
DOI: doi:10.3791/4201

Keywords: Medicine, Issue 69, Neuroscience, Cancer Biology, Stem Cell Biology, Bioengineering, Biomedical Engineering, polished and reinforced thin-skull cranial window, two-photon microscopy, glioma stem cell, vasculature, PoRTS

Date Published: 11/20/2012

Citation: Zhang, L., Lapierre, A., Roy, B., Lim, M., Zhu, J., Wang, W., Sampson, S.B., Yun, K., Lyons, B., Li, Y., Lin, D. Imaging Glioma Initiation *In Vivo* Through a Polished and Reinforced Thin-skull Cranial Window. *J. Vis. Exp.* (69), e4201, doi:10.3791/4201 (2012).

Abstract

Glioma is the one of the most lethal forms of human cancer. The most effective glioma therapy to date-surgery followed by radiation treatment-offers patients only modest benefits, as most patients do not survive more than five years following diagnosis due to glioma relapse [1,2]. The discovery of cancer stem cells in human brain tumors holds promise for having an enormous impact on the development of novel therapeutic strategies for glioma [3]. Cancer stem cells are defined by their ability both to self-renew and to differentiate, and are thought to be the only cells in a tumor that have the capacity to initiate new tumors [4]. Glioma relapse following radiation therapy is thought to arise from resistance of glioma stem cells (GSCs) to therapy [5-10]. *In vivo*, GSCs are shown to reside in a perivascular niche that is important for maintaining their stem cell-like characteristics [11-14]. Central to the organization of the GSC niche are vascular endothelial cells [12]. Existing evidence suggests that GSCs and their interaction with the vascular endothelial cells are important for tumor development, and identify GSCs and their interaction with endothelial cells as important therapeutic targets for glioma. The presence of GSCs is determined experimentally by their capability to initiate new tumors upon orthotopic transplantation [15]. This is typically achieved by injecting a specific number of GBM cells isolated from human tumors into the brains of severely immuno-deficient mice, or of mouse GBM cells into the brains of congenic host mice. Assays for tumor growth are then performed following sufficient time to allow GSCs among the injected GBM cells to give rise to new tumors-typically several weeks or months. Hence, existing assays do not allow examination of the important pathological process of tumor initiation from single GSCs *in vivo*. Consequently, essential insights into the specific roles of GSCs and their interaction with the vascular endothelial cells in the early stages of tumor initiation are lacking. Such insights are critical for developing novel therapeutic strategies for glioma, and will have great implications for preventing glioma relapse in patients. Here we have adapted the PoRTS cranial window procedure [16]and *in vivo* two-photon microscopy to allow visualization of tumor initiation from injected GBM cells in the brain of a live mouse. Our technique will pave the way for future efforts to elucidate the key signaling mechanisms between GSCs and vascular endothelial cells during glioma initiation.

Video Link

The video component of this article can be found at http://www.jove.com/video/4201/

Protocol

1. Protocol

1. Anesthetize the mouse with ketamine and xylazine at a dose of 0.1 mg ketamine and 0.01 mg of xylazine per 1 g of body weight. Carprofen (0.005 mg per 1 g of body weight) is used for analgesia and is administered preoperatively.
2. All of the surgical tools, including the dental drill bit, are steam sterilized in an autoclave. If batch surgeries are to be performed, the tips of surgical instruments must be re-sterilized with a glass bead sterilizer (Fine Science Tools FST 250) before each subsequent surgery.
3. Once the mouse has reached a surgical plane of anesthesia, assessed by absence of a response to a toe pinch, it is placed on a cotton pad that is then placed on a heated pad to maintain a body temperature of ~37 °C. The depth of anesthesia is monitored frequently during the surgery.
4. Fur is removed from the dorsal head in a roughly triangular area ~ 3 mm caudal to the nares and extending caudally to the cervical vertebrae. Ophthalmic ointment is applied to eyes to protect them from dehydration and irritation.
5. The mouse is placed in ventral recumbancy and the skin is disinfected with surgical iodine, 70% ethanol, and sterile swabs. A 0.8 x 1.0 cm flap of skin covering the dorsal aspect of the frontal and parietal bones of the skull is removed using fine scissors.
6. A topical analgesic, 0.5% lidocaine, is applied locally to the periosteum and the exposed tissues at the periphery of the wound. The periosteum is removed by gently scraping the skull with a scalpel blade; this will help the cyanoacrylate glue to adhere to the bone.

Copyright © 2012 Journal of Visualized Experiments

7. The cortical area of interest is outlined on the skull with a marker. The area of interest should not be located over skull suture lines, to avoid damage to underlying large vessels.
8. A thin layer of cyanoacrylate adhesive is applied to the wound margins, to prevent the seepage of serosanguinous fluid, and to the skull except in the area of interest.
9. Light-activated dental cement is used in our protocol for sealing the skull. Before application of dental cement, all exposed skull except for the area intended for thinning is treated with the primers and subsequently with the bonding agent from the light-activated dental cement kit. Once the bonding agent is dried, the light-activated dental cement is applied to cover the skull. To stabilize the head of the mouse for subsequent surgery and imaging, a sterile #00-90 hex nut is embedded into the dental cement at a distance from the area to be thinned. The use of light- activated dental cement allows us to prepare the skull without having to rush to finish the entire procedure. Once the dental cement preparation on the skull is completed, the dental cement is cured with visible light.
10. After the dental cement is cured, a headpiece holder from the stereotactic device is mounted to the hex nut on the mouse head using a #00-90 screw.
11. A drop of room-temperature, 0.9% sterile saline is applied to the skull area to be thinned. With the aid of a stereomicroscope, a high-speed micro-drill is used to thin a circular area of the skull (typically ~4-5 mm in diameter) over the region of interest. Drilling and the application of saline to the drilled area are performed intermittently during the thinning procedure to avoid thermal injury to the underlying cerebral tissue. Saline absorbs heat and also helps soften the bone.
12. The mouse skull comprises two thin layers of compact bone, sandwiching a thick layer of spongy bone. The external layer of compact bone and most of the spongy bone are removed using the drill.
13. After the majority of the spongy bone is removed, the remaining cavities within the spongy bone can be seen under a dissecting microscope, indicating that drilling is approaching the internal compact bone layer. At this stage, skull thickness should still be more than 50 µm. Skull thinning should be continued carefully to obtain a very thin (~20 µm) and smooth preparation.
14. Once the desired thickness of skull is achieved (~20 µm), the skull is first polished using a custom-made silicone whip with diamond paste (6-15 µm) for approximately 10 min. The diamond-paste polishing serves two purposes. First, it further thins the skull without applying pressure on the thinned skull, thereby avoiding accidental damage to the underlying brain tissue. Second, it serves as an initial polishing step for the thinned skull before the fine-grained tin oxide is used for further skull polishing.
15. Following the diamond-paste polishing, the thinned skull is polished with tin oxide for approximately 10 min. Once the skull is polished, the tin oxide is flushed away with saline until the thinned skull appears clean.
16. At this step, if the cranial window is to be used for longitudinal *in vivo* imaging, the cleaned thin skull area is dried. A small drop of clear cyanoacrylate glue is applied to seal the cranial window. The layer of cyanoacrylate glue between the thinned skull and the coverslip should be as thin as possible.
17. If an injection is to be performed after creation of a PoRTS cranial window, at this step, a 26-gauge syringe needle is used to create a small opening on one side of the polished thin-skull window. This opening is used for GBM cell injection.
18. A sterile glass pipette with a tip opening approximately 50 µm in diameter is pulled using a pipette puller. This pipette will be used for GBM cell injection, and is loaded onto a micromanipulator. The pipette is loaded at a 30-degree angle so that the GBM cell injection site will be away from the final imaging site. The tip of the pipette is removed under a dissection microscope. The GBM cell suspension is front-loaded into the pipette by suction using a syringe pump.
19. Once the injection pipette is loaded with GBM cells, the mouse is moved back under the microscope. The injection pipette is lowered towards the small opening in the cranial window and finally inserted into the brain through the opening using a micromanipulator. 1 µl of a GBM cell suspension is injected into the brain 100-200 µm from the brain surface (speed: 0.1 µl/min, duration: 10 min).
20. The skull is dried, a small drop of clear cyanoacrylate glue is applied to the dried skull, and a piece of 3-mm size #1 coverslip is adhered to the thin and polished skull area. The space between the coverslip and adjacent dental cement is sealed with cyanoacrylate glue.
21. After surgery, the mouse is injected subcutaneously with 1 ml warm sterile saline and provided with supplemental heat to maintain body temperature until fully recovered from anesthesia.
22. For imaging, mice are anesthetized with ketamine and xylazine at a dosage of 0.1 mg ketamine and 0.01 mg of xylazine per 1 g of body weight. Mice are immobilized using a custom stereotactic frame under the microscope. If repetitive *in vivo* imaging is performed on daily basis, isofluorane will be a better option, as mice will show signs of dependence with repetitive use of ketamine.

2. Representative Results

A successful PoRTS cranial window surgery allows the cranial window to remain clear for weeks to months. **Figure 1** shows the vasculature beneath a PoRTS cranial window as visualized using backscattered light. These vasculature images were used as landmarks for locating the same brain areas for repetitive imaging. To visualize both the vasculature endothelial cells and GBM cells, we crossed the B6.Cg-Tg(Tek-cre)1Ywa/J mouse, which labels vascular endothelial cells with the B6.Cg-Gt(ROSA)26Sor$^{tm9(CAG\text{-}tdTomato)Hze}$/J mouse, and generated mice with vascular endothelial cells labeled with the red fluorescent protein tdTomato. We then performed the PoRTS craniotomy procedure on these mice, and injected GFP-labeled GBM cells into their brains through a small opening on the side of a cranial window. We then performed *in vivo* two-photon imaging longitudinally on the injected mice. The laser excitation wavelength was set at 910 nm, which resulted in excitation of both GFP and tdTomato. Two-photon imaging was performed on a custom-built two-photon laser-scanning microscope with two detectors for simultaneous green/red fluorescence detection capability. **Figure 2** shows an *in vivo* example of glioma initiation from injected GBM cells near the vasculature. The PoRTS cranial window is also an excellent choice for chronic time-lapse *in vivo* imaging. **Figure 3** shows GFAP staining of cortical sections from a mouse without PoRTS surgery, a mouse 7 days following PoRTS surgery, and a mouse 7 days following PoRTS surgery and saline injection. It is evident from the images that the mouse without surgery and the mouse with PoRTS surgery do not have gliosis, whereas following saline injection, gliosis is observed in the brain tissue of the mouse, due to pipette penetration and saline injection in the brain. This result demonstrates that gliosis does not occur under the PoRTS cranial window, providing independent validation that the PoRTS cranial window described here does not lead to the gliosis that is typically associated with an "open skull" chronic cranial window. **Figure 4** shows high-resolution imaging of dendritic spines from the same mouse on the day of surgery (Day 0) and 32 days after the PoRTS window creation (Day 32), demonstrating that the PoRTS window is also an excellent choice for high-resolution *in vivo* imaging.

Copyright © 2012 Journal of Visualized Experiments

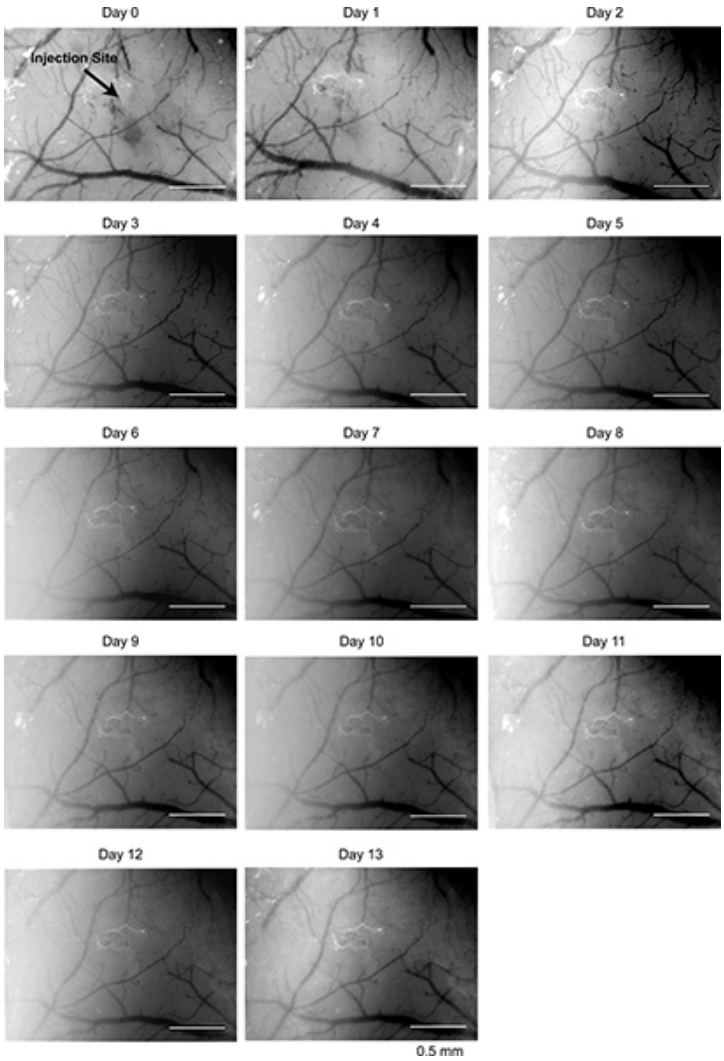

Figure 1. Visualization of vasculature under a polished and reinforced thinned skull cranial window using backscattered light. Days represent the number of days after surgery; images were taken starting on the day of surgery immediately after completion of GBM cell injection. Scale bar: 0.5 mm. Click here to view larger figure.

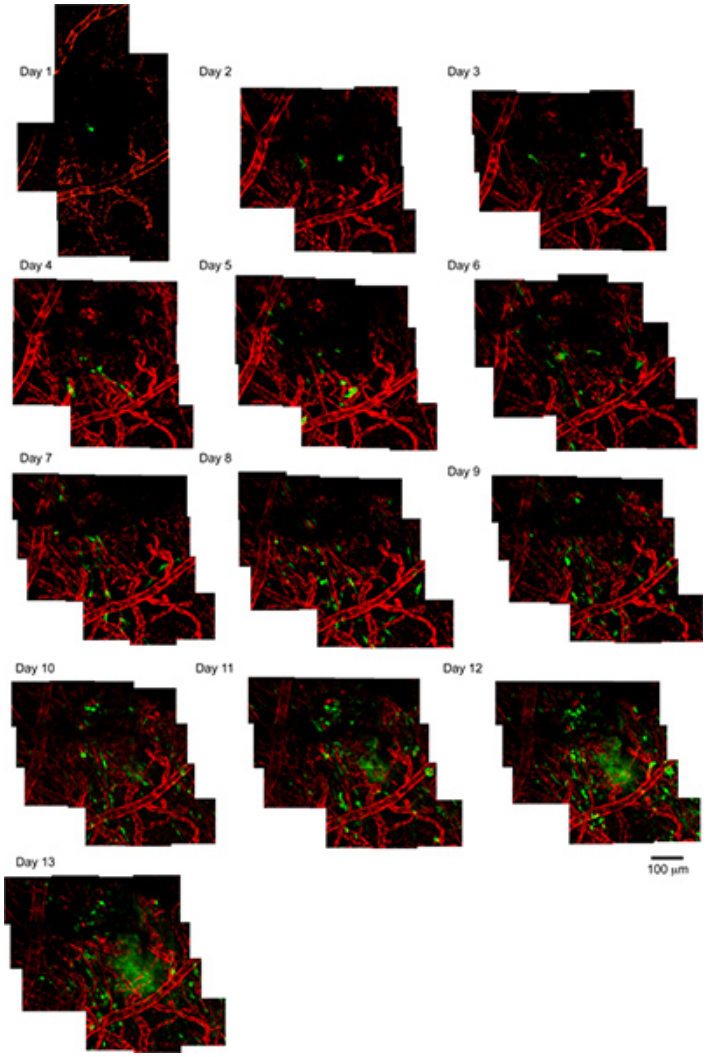

Figure 2. Visualization of injected GBM cells and vasculature *in vivo*. Mice carrying both Tek-Cre and ROSA26 CAG-tdTomato were used for GBM cell injection. Vascular endothelial cells were labeled with tdTomato (red), and GBM cells were labeled with GFP (green). Images were acquired starting 24 hr after GBM cell injection. A total of 10-12 adjacent fields of view were taken and were assembled adjacent to one another, with the identified injected GBM cells in the center of the total field, to produce the final images. Days represent the number of days after surgery. Scale bar: 100 µm. Click here to view larger figure.

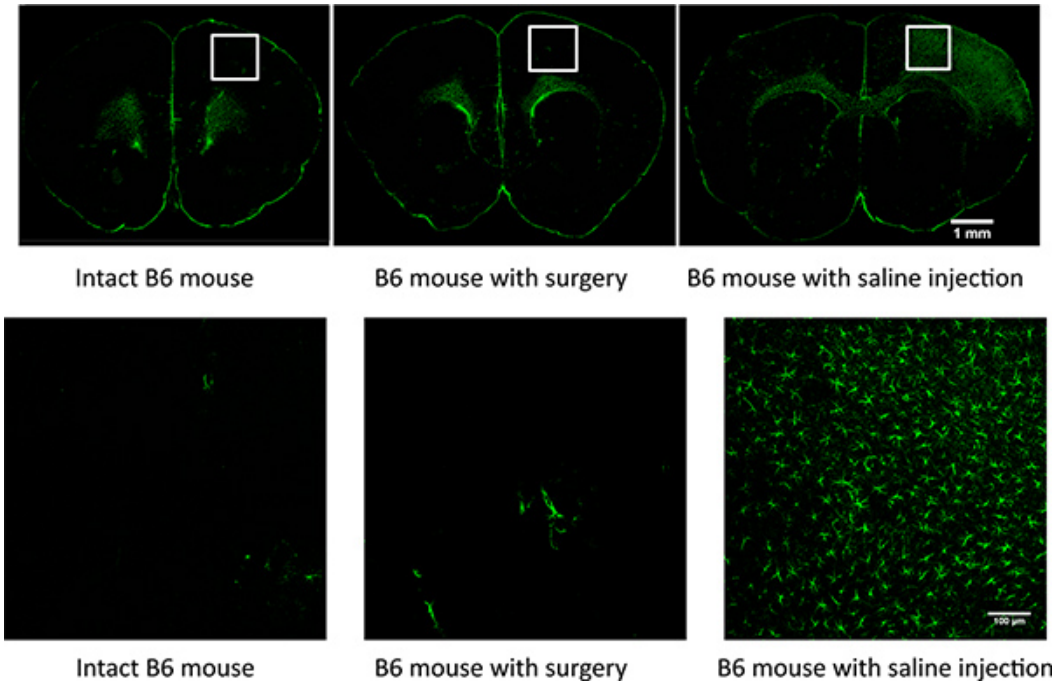

Figure 3. Gliosis does not occur following PoRTS cranial window surgery. Upper panels: Mouse brain coronal section under lower magnification. Left panel: a mouse without any cranial window surgery; no GFAP activation is observed in the brain tissue. Middle panel: a mouse with a PoRTS cranial window generated on the right side of the brain; no GFAP activation is observed in the brain tissue. Right panel: a mouse with a PoRTS cranial window and saline injection from the side of the PoRTS window. GFAP activation is observed on the side of the PoRTS window, but not on the side of intact brain tissue. Scale bar: 1 mm. Lower panel: higher-power images of brain tissues in areas as indicated in the white box of the upper-panel images. Scale bar: 100 µm. Click here to view larger figure.

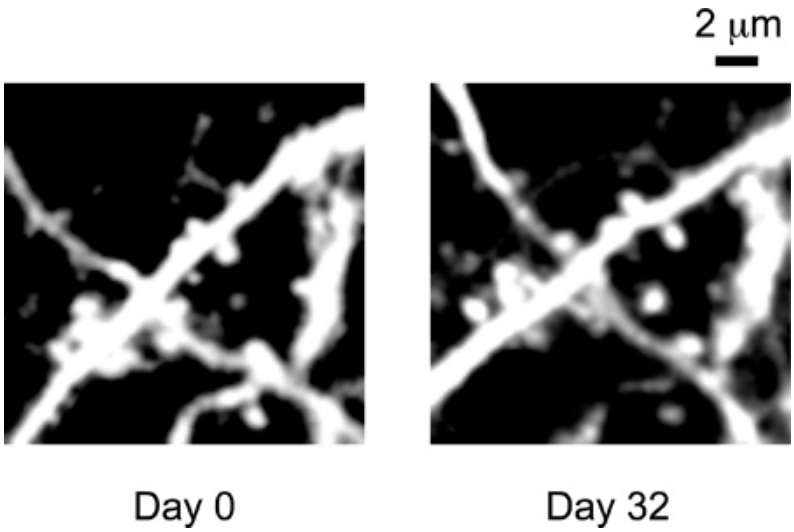

Figure 4. High-resolution imaging of dendritic spines from Thy-1 YFPH mice. Images were acquired on the day of PoRTS surgery, and 32 days after PoRTS surgery. It is apparent from the images that most spines present on day 0 are clearly visible 32 days following PoRTS surgery. Scale bar: 2 µm.

Discussion

The key to a successful PoRTS cranial window is the thinning and polishing. While the initial thinning can be performed quickly, care should be taken to ensure homogenous thinning of the skull over a large area. We typically apply a thin layer of saline to the skull, and then thin the skull one pass at a time, such that the saline solution evaporates shortly after the microdrill has passed over the skull once. This allows us to slowly but homogenously further thin the skull. A steady hand under the microscope is also key. Once skull-thinning nears the intended thickness, we normally use diamond paste to polish the thinned skull for 10-15 min, with subsequent polishing using tin oxide. We find that polishing the

thinned skull first with diamond paste yields a better polishing result in general, and also allows us to further thin a large area of skull area without applying much pressure onto the thinned skull area.

We chose the PoRTS cranial window rather than other commonly used cranial windows, such as the "open skull" window and the "thinned skull" window, for the following reasons: With the open skull window, the cranial window usually becomes cloudy shortly after creation and then clears up on its own within the first two weeks, thus requiring a waiting period of approximately two weeks before any imaging experiments can be performed. This two-week waiting period would prevent visualization of glioma initiation during the initial two weeks following GBM cell injection. The thinned skull cranial window requires repetitive thinning before each imaging session, which renders it unsuitable for GBM cell injection and visualization of glioma initiation on a daily basis. In contrast, the PoRTS window allows us to perform GBM cell injection from the side of the window, which minimizes damage to the brain tissue, and also allows for performance of high-resolution imaging immediately following creation of the window. Information on glioma initiation can be collected within the first few weeks following GBM cell injection, which is a key advantage over the open skull technique for this type of studies.

Disclosures

No conflicts of interest declared.

Acknowledgements

This work is supported by The Jackson Laboratory Cancer Center Pilot Grant and The Maine Cancer Foundation.

References

1. Paulino, A.C. & Teh, B.S. Treatment of brain tumors. *N. Engl. J. Med*. **352**, 2350-2353, author reply 2350-2353 (2005).
2. Stupp, R., *et al.* Radiotherapy plus concomitant and adjuvant temozolomide for glioblastoma. *N. Engl. J. Med.* **352**, 987-996 (2005).
3. Singh, S.K., *et al.* Identification of human brain tumour initiating cells. *Nature.* **432**, 396-401 (2004).
4. Hanahan, D. & Weinberg, R.A. Hallmarks of cancer: the next generation. *Cell.* **144**, 646-674 (2011).
5. Cheng, L., Bao, S., & Rich, J.N. Potential therapeutic implications of cancer stem cells in glioblastoma. *Biochem. Pharmacol*. **80**, 654-665 (2010).
6. Cheng, L., Ramesh, A.V., Flesken-Nikitin, A., Choi, J., & Nikitin, A.Y. Mouse models for cancer stem cell research. *Toxicol. Pathol.* **38**, 62-71 (2010).
7. Dirks, P.B. Brain tumor stem cells: the cancer stem cell hypothesis writ large. *Mol. Oncol.* **4**, 420-430 (2010).
8. Ebben, J.D., *et al.* The cancer stem cell paradigm: a new understanding of tumor development and treatment. *Expert Opin. Ther. Targets.* **14**, 621-632 (2010).
9. Germano, I., Swiss, V., & Casaccia, P. Primary brain tumors, neural stem cell, and brain tumor cancer cells: where is the link? *Neuropharmacology.* **58**, 903-910 (2010).
10. Park, D.M. & Rich, J.N. Biology of glioma cancer stem cells. *Mol. Cells.* **28**, 7-12 (2009).
11. Bao, S., *et al.* Stem cell-like glioma cells promote tumor angiogenesis through vascular endothelial growth factor. *Cancer Res*. **66**, 7843-7848 (2006).
12. Calabrese, C., *et al.* A perivascular niche for brain tumor stem cells. *Cancer Cell*. **11**, 69-82 (2007).
13. Barami, K. Relationship of neural stem cells with their vascular niche: implications in the malignant progression of gliomas. *J. Clin. Neurosci*. **15**, 1193-1197 (2008).
14. Gilbertson, R.J. & Rich, J.N. Making a tumour's bed: glioblastoma stem cells and the vascular niche. *Nat. Rev. Cancer*. **7**, 733-736 (2007).
15. Cho, R.W. & Clarke, M.F. Recent advances in cancer stem cells. *Curr. Opin. Genet. Dev.* **18**, 48-53 (2008).
16. Drew, P.J., *et al.* Chronic optical access through a polished and reinforced thinned skull. *Nat. Methods*. **7**, 981-984 (2010).

Copyright © 2012 Journal of Visualized Experiments